Chalcogenide Letters Vol. 9, No. 1, January 2012, p. 41 - 50

OPTICAL PROPERTIES AND I-V CHARACTERISTIC CURVE OF CHALCOGENIDE AMORPHOUS Ge–Sb–Te FILMS

AFAF A. ABD EL-RAHMAN[a], - F. M. HAFEZ[a], F. AHMAD[a], M. M. ELOKR[b]
[a]*Physics Department, Faculty of Science, Al-Azhar University, Girls branch, Cairo, Egypt.*
[b]*Physics Department, Faculty of Science, Al-Azhar University, Cairo, Egypt.*

The optical properties of solid films of chalcogenide glass system Ge-Sb-Te were investigated. Elemental composition of the two investigated samples is determined by the energy dispersion X-ray technique. They were found to be Ge_5 Sb_{32} Te_{63} and Ge_9 Sb_{27} Te_{64}, denoted by C1 and C2, respectively. The influences of composition and film thickness on the optical band gap (E_o) were investigated at room temperature. This was done by an analysis of transmittance (T) and reflection (R) spectra in the fundamental absorption region. It was found that the magnitude of E_o decreases with increasing Ge content. The obtained results were interpreted in terms of the change of cohesive energy (C.E.) as a function of Ge content. The cohesive energy was estimated by employing the chemical bond approach. Temperature dependent measurements of the electrical resistance of the films for composition C1 and C2 in the temperature range 300-473 K were performed. The obtained result showed rapid transition from high resistance state to low resistance state. The observed transition temperature for composition C1 is lower than that for C2, with higher Ge content and hence higher cohesive energy. I-V characteristic curves for compositions C1 and C2, at 300 nm thickness indicate that, composition C1 may be used as read-write material and C2 as read-rewrite material.

(Received October 18, 2011; Accepted January 13, 2012)

Keywords: Ge–Sb–Te, chalcogenide, thin film

1. Introduction

In recent years, chalcogenide alloys have received considerable attention because of their wide ranging applications in infrared transmission, semiconductors, photovoltaics and in phase-change recording technology [1-3]. GeSbTe amorphous films are widely used in rewritable compact disks (CD-RW), digital versatile disks (DVD-RW) and are found to be suitable for electrical memories (i.e. non-volatile memories). In optical applications, information is recorded using the fact that a thin film of this system can be reversibly switched by laser heating between the amorphous and the crystalline state [4-9].

The present study was undertaken in order to investigate:- 1) the influences of composition and film thickness on the optical properties of chalcogenide glass compositions Ge_5 Sb_{32} Te_{63} and Ge_9 Sb_{27} Te_{64}, denoted by C1 and C2, respectively at room temperature. The obtained results were tentatively interpreted in terms of the chemical bond approach [10] used to estimated the cohesive energy of the glasses under investigation. 2) To study the temperature dependence of electrical resistance and I-V characteristic curves for two investigated composition.

2. Experimental techniques

Glass composition Ge_5 Sb_{32} Te_{63} and Ge_9 Sb_{27} Te_{64} were prepared from highly pure element Ge, Sb and Te (99.999% purity). These constituents were weighted in accordance with their atomic percentages. The materials for each composition were placed into a silica tube. The tubes were sealed in a vacuum of 10^{-4} Torr and heated in a muffle furnace at about 1000 ^{o}C for 12 hours and shaken several times during the course of heating to ensure a high degree of homogeneity. The melt was quenched in ice water.

Film samples having thickness of 300, 200, 150, and 70 nm was prepared for the two compositions. Films were deposited by thermal evaporation technique onto thoroughly cleaned glass substrates using a high vacuum coating unit model (Edwards E 306-A) the deposition temperature was maintained at room temperature. The pressure inside the vacuum chamber was brought down to ≈ 10^{-3} Torr using the rotary pump. The evacuation was then contained using oil diffusion pump until the vacuum reaches≈ 10^{-5} Torr before deposition. Digital film thickness monitor (Maxtex Inc. model TM200Sin 531) adjusted the rates of evaporation and film thickness. All films have been annealed at 433 K for two hours.

The samples were examined before and after annealing using Philips Analytical X-Ray diffraction system, type PW3710 with Cu anode of wave length $K\alpha_1$ = 1.5460 $\AA$ and $K\alpha_2$ = 1.54439 $\AA$. The generator tension was 40 kV and the generator current was 30mA. The start angle 2θ was 10 degrees and the end angle was 100 degrees for bulk sample and 70 degrees for films.

The reflection and transmission of the prepared films were measured in spectral range 300-1100 nm using PMQII carl Zeiss spectrometer supplied with a reflection attachment. The errors in these measurements (reflection and transmission) did not exceed 0.01 ev.

For electrical measurements, the samples were in the form films with silver electrodes. D.C. resistance as a function of temperature was measured using Keithly 485 Autoranging picoammeter and digital multimeter M 3922.

3. Results and discussion

3.1. X-ray

X-ray diffraction patterns of the investigated films of thicknesses (300, 200, 150 and 70 nm) of the two compositions, C1 and C2 are illustrated in figures 1 and 2, respectively. No diffraction peaks are present, reflecting the amorphous nature of the prepared films. The above mentioned films were subjected to annealing at a temperature of 433 K for two hours, and then allowed to cool slowly in the oven. The X-ray patterns of the annealed films are presented in figures 1 and 2. It is apparent that, the films of the investigated compositions still have an amorphous structure. However, annealing films exhibit humps, which may be related to the formation of small crystallites.

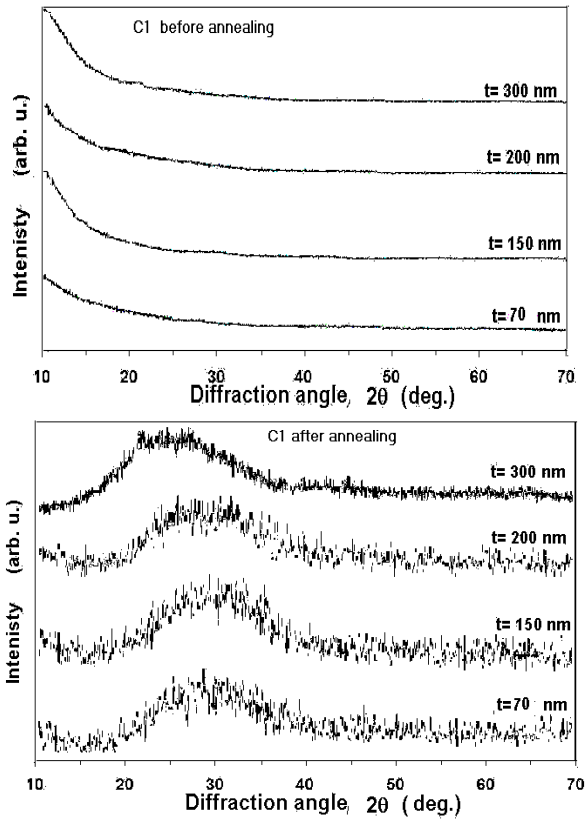

Fig. 1 X-ray diffraction pattern of the composition C1, before and after annealing, for different thicknesses.

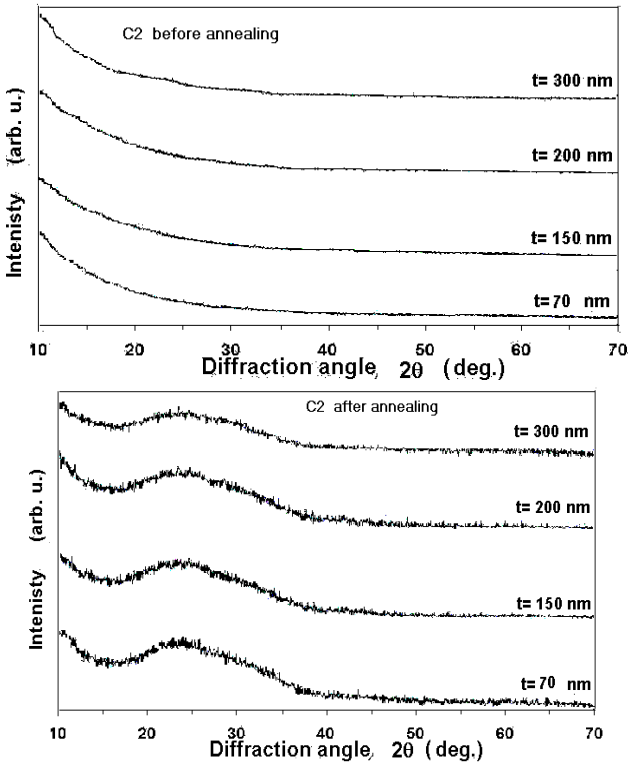

Fig. 2 X-ray diffraction pattern of the composition C2, before and after annealing, for different thicknesses.

3.2. Optical band gap determination

For the determination of the optical band gap, E_o, the procedure suggested by De Michelis et al [11] was used. Near the absorption edge, R and T are related to absorption coefficient, α, by

$$T = (1-R) \exp(-\alpha t) \quad (1)$$

where t is the thickness of the film sample, then

$$\alpha = (1/t) \, \mathrm{Ln} \{(1-R)/T\} \quad (2)$$

By measuring R and T at different wavelengths, α can be estimated. The spectral dependence of the absorption coefficient has the form [11]

$$\alpha\hbar\omega = A (\hbar\omega - E_o)^n \quad (3)$$

where ħω is the photon energy, E_o is the optical band gap and n is a parameter depending on both the type of transition (direct or indirect) and the profile of the electron density in the valence and conduction bands. Here, A is a constant including the thickness t. It should be pointed out that this method eliminates the errors arising from the uncertainty in thickness determination.

The dependence of $(\alpha\hbar\omega)^{1/n}$ on the photon energy ħω was plotted for different values of n. the best fit was found to be with n=2. This is the characteristic behavior of indirect transition in non-crystalline material. Figures 3 and 4 show the dependence of $(\alpha\hbar\omega)^{1/2}$ against ħω for all films before and after annealing for investigated compositions C1 and C2, respectively. The estimated values of E_o obtained from these curves are listed in table 1.

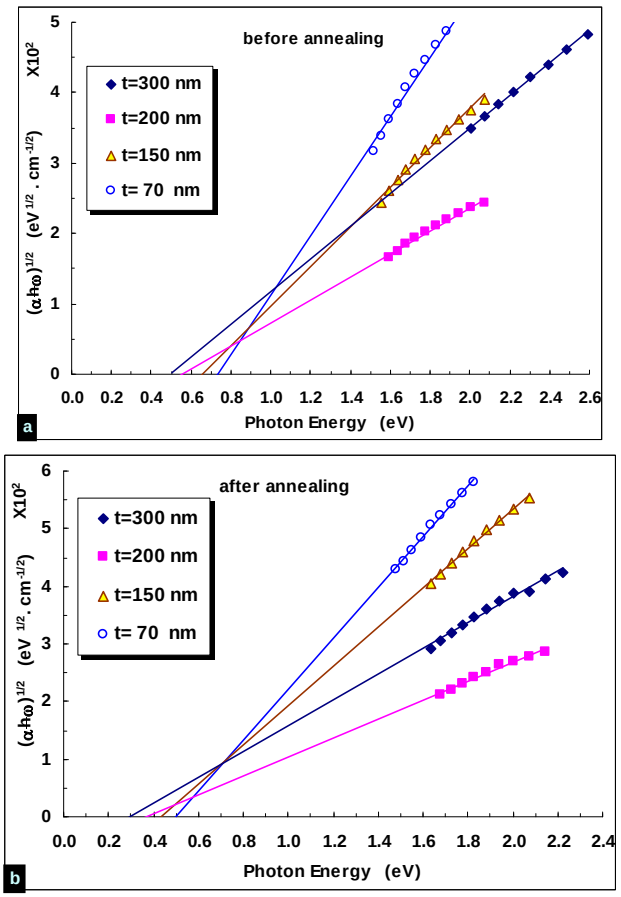

Fig. 3 $(\alpha\hbar\omega)^{1/2}$ against photon energy for composition C1, a) before annealing, b) after annealing, for different thicknesses.

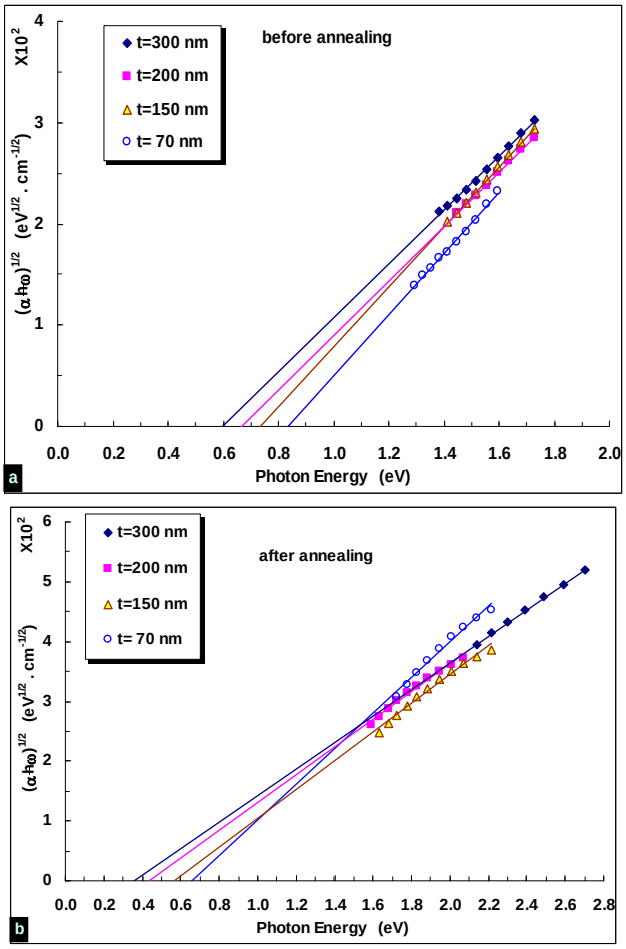

Fig. 4 $(\alpha\hbar\omega)^{1/2}$ against photon energy for composition C2, a) before annealing, b) after annealing, for different thicknesses.

Table 1 Estimated values of E_o with the calculated values of C.E. for the two compositions C1 and C2 before and after annealing for different thicknesses.

Thickness (nm)		Before annealing E_o (eV)	After annealing E_o (eV)	C.E (eV/atom)
C1	300	0.49	0.30	1.83
	200	0.55	0.37	
	150	0.66	0.43	
	70	0.74	0.50	
C2	300	0.60	0.35	1.89
	200	0.67	0.44	
	150	0.73	0.57	
	70	0.84	0.67	

As seen in table 1 the value of the optical band gaps increase with increasing Ge content. This variation of the E_o as a function of Ge content may be explained in terms of the change in cohesive energy (C.E.) as a function of Ge content. It might be possible to assume that the observed change in optical properties upon annealing is a result of micro structural re-arrangement

occurs during annealing. To test the validity of this argument, the cohesive energies of the investigated compositions were calculated using the method suggested by the chemical bond approach [10]. This is done by first considering the types of bonds expected to occur in the present compositions to an appreciable extent [12]. These are presented in table 2 together with their bond energies.

Table 2 Calculated values of the bond energies expected to occur in C1 and C2 compositions.

(C-D)	*H(C-D) kcal/mole*
Ge-Te	35.5
Sb-Te	31.6
Sb-Sb	30.2

The bond energy H(C-D) for heteronuclear bonds was calculated using the formula [13]

$$H\,(C\text{-}D) = \{H\,(C\text{-}C)\,.H\,(D\text{-}D)\}^{1/2} + 30\{Y_C\text{-}Y_D\}^2 \qquad (4)$$

H(C-C) and H (D-D) are the energies of the homo-nuclear bonds. The H (C-C) values are in units of kcal/mole: 37.6 for Ge, 33 for Te and 30.2 for Sb. Y_C and Y_D are the electro negativities of the atoms involved. The Y values used are 2.01 for Ge, 2.1 for Te and 2.05 of Sb [14].

Bonds are formed in the sequence of decreasing bond energy until all the available valance of the atoms is satisfied [15]. In the present compositions, the Ge-Te bonds with the highest possible energy (35.5 kcal/mole) are expected to saturate all available valences of Te. The fairly strong Sb-Te bond (31.6 kcal./mole) is not expected to occur. There is still unsatisfied Sb valences, which must be satisfied by the formation of Sb-Sb defect homo-polar bonds for the two compositions C1and C2. Based on the chemical bond approach, the bond energies are assumed to be additive. Thus, the cohesive energies were estimated by summing the bond energies listed in table 2 over all the bonds expected in the material. These results indicate that the C.E. of these glasses shows an increase with increasing Ge content. Therefore, it can be concluded that the increase of E_o with increasing Ge content are most probably due to the increase of the average stabilization energy by Ge addition. This conclusion is consistent with the optical measurements reported earlier [16].

3.3. Temperature dependence of the electrical resistance

Figs. 5 and 6 show plots of the temperature dependence of resistance R(T) in the temperature range 300-473 K, for all films of the investigated compositions C1 and C2, respectively. As seem from these figures, all plots exhibit a rapid transition between high resistance to low resistance state. For example, the values of R (T) at the transition temperature (for 300 nm thickness) are two and four orders of magnitude higher than its value before transition, for C1 and C2, respectively. For composition C1, the sudden change occurs at transition temperatures around 417, 410, 405, and 391 K for thicknesses 300, 200, 150 and 70 nm, respectively. For composition C2, the transition occurs at transition temperatures around 432, 425, 412 and 397 K for thicknesses of 300, 200, 150 and 70 nm, respectively. It should be noted that, the observed transition temperature depends on both composition and film thickness. Transition temperatures increase by increasing both Ge content and thickness. Such it might is related to structural changes.

To identify resistance changes as reversible or irreversible, films subjected to cyclic heating. Subsequent cooling leads to an irreversible change in the film's resistance. This irreversible change in R(T) suggests the ability of these compositions to be used as memory device.

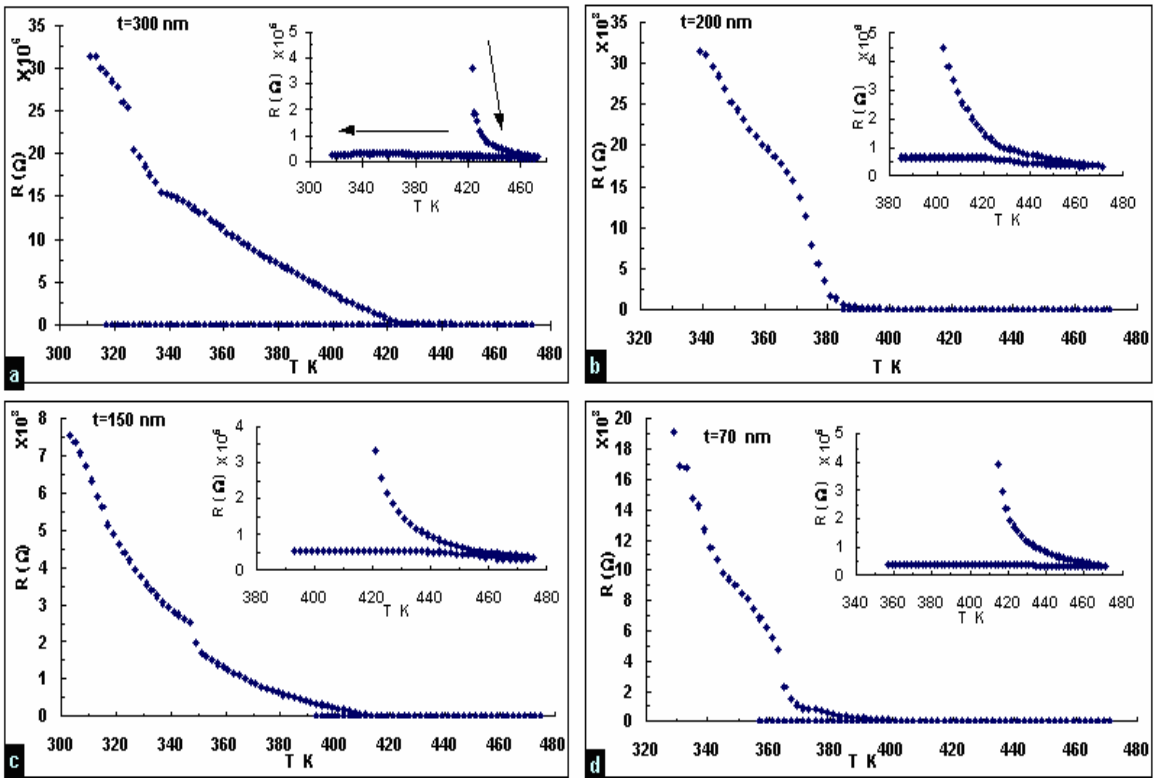

Fig. 5 D.C.resistance against temperature for composition C1 before annealing.

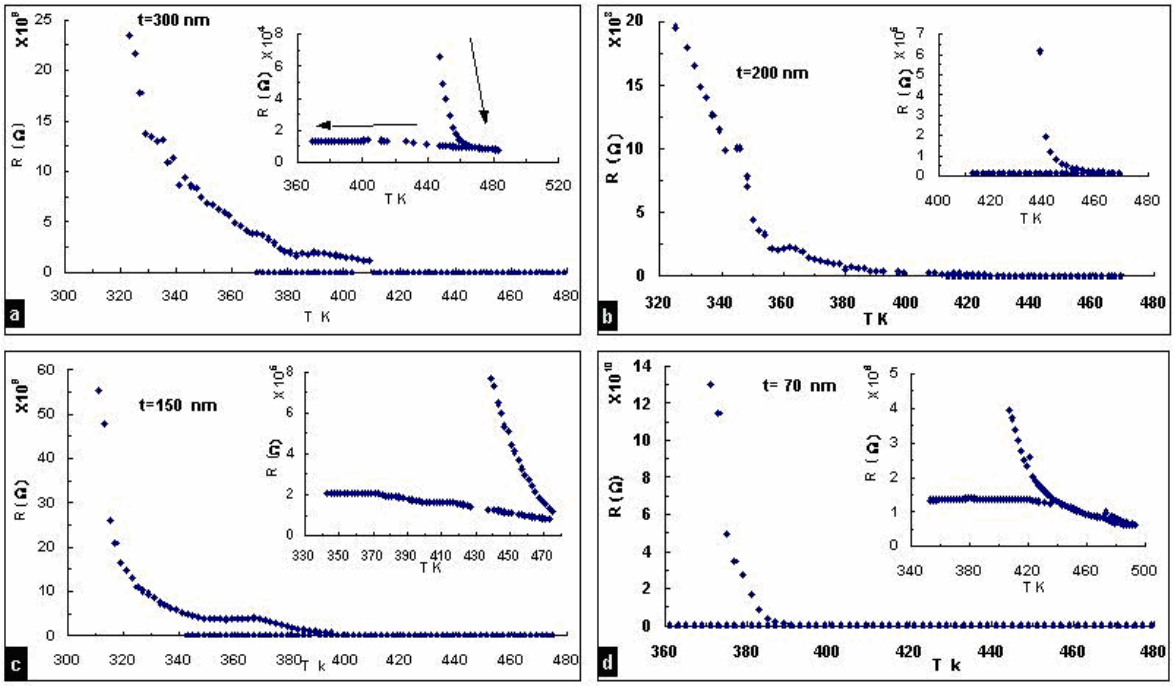

Fig. 6 D.C.resistance against temperature for composition C2 before annealing.

3.4. I-V characteristic curve

The room temperature static hysteresis I-V characteristic curve for compositions C1 and C2 at 300 nm thickness are presented in figures 7 and 8. It is observed that increasing the applied voltage up to threshold voltage, V_{th} , at a pinot (b), a very small current is obtained (ab) which represent the OFF state (high resistance) of the switch. At a point (b) the sudden increase in current takes place (ON state). Therefore, no data points were taken in this range (bc). A further

increase in the applied voltage increases the current (cd). By decreasing the applied voltage the current decreases until finally both become zero (da of the curve). This curve is atypical hysteresis I-V characteristic for memory switch.

If second pulse applied on this investigated film sample, C1 will remains in ON state. This behavior may be used as read -write material. On other hand, C2 exhibit the two states (OFF and ON state) after each cycles. This suggests the use of C2 film as read – rewrite material.

It is noticed that, investigated thickness of composition C1 has V_{th} is less than that in composition C2. It can be accounted for by considering that C.E. of C1 is less than it for C2.

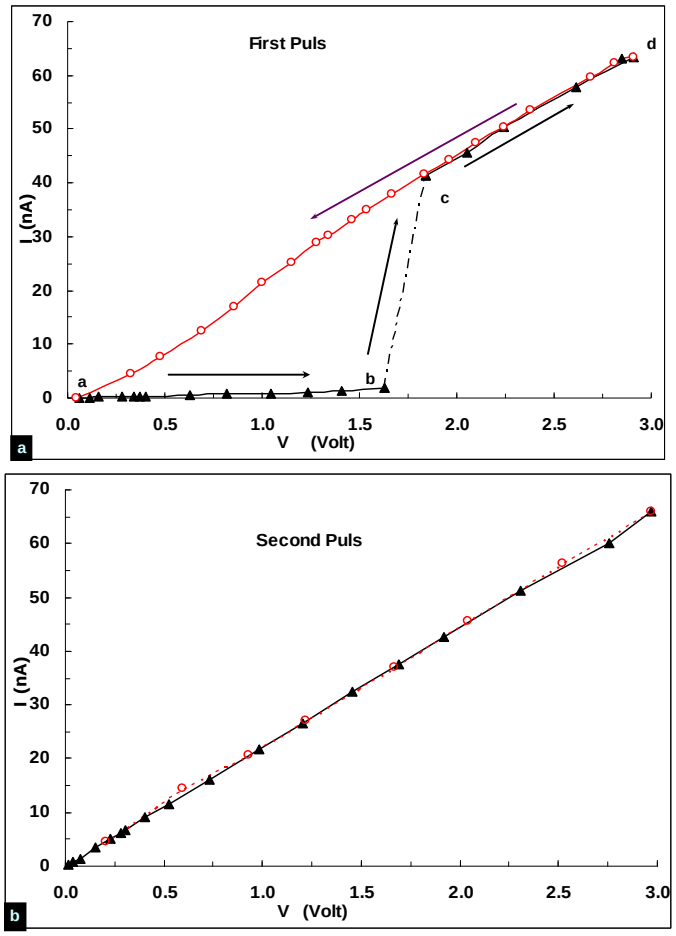

Fig. 7 Hystersises I-V charactristic curve for composition C1 before annealing at thickness 300 nm (a) first measurement (b) second measurement.

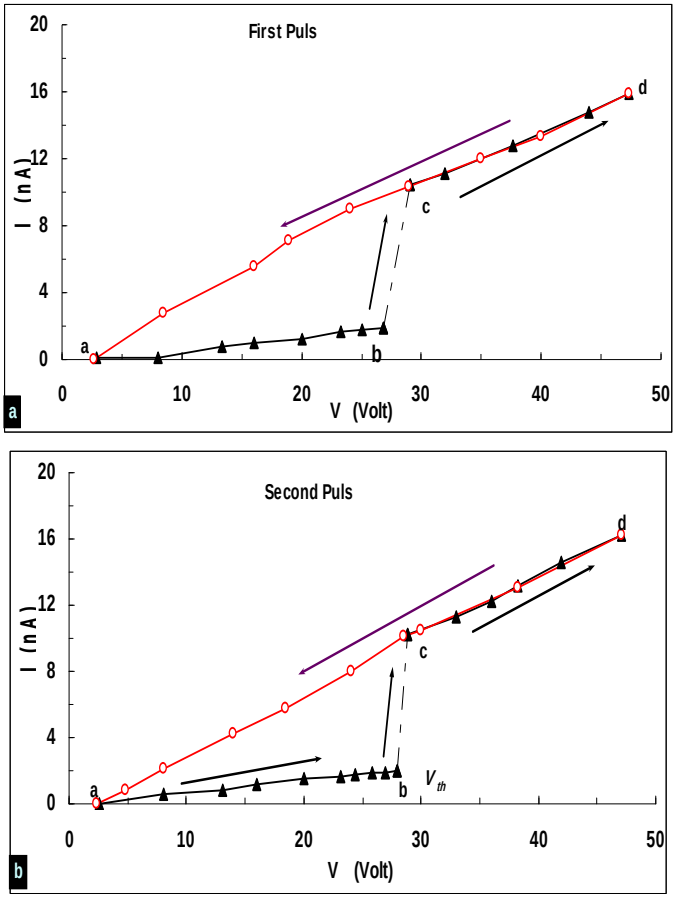

Fig. 8. Hysteresis I-V characteristic curve for composition C2 before annealing at thickness 300 nm (a) first measurement (b) second measurement.

4. Conclusion

No diffraction peaks were observed in the X-ray pattern of the investigated films before and after annealing indicating their amorphous nature. Optical energy gap (E_o) was found to increase with increasing Ge content. These results were explained in terms of the change of C.E as a function of Ge content. The optical band gap was found to decrease with increasing thickness, before and after annealing, and decrease in its value upon annealing. From hysteresis I-V characteristic curves it was concluded that, the composition Ge_5 Sb_{32} Te_{63} may be used as read-write material, however Ge_9 Sb_{27} Te_{64} can be read-rewrite material

References

[1] V. Weidenhof, P. Franz and M. Wuttig J. of Appl. Phys., **87**, 9 (2000).
[2] J. S. Sanghera, J. Heo and J. D. J. Machkenzie, J. of Non-Cryst. Solid, **103**, 155 (1988).
[3] D. Wamwangi, W.K. Njoroge, M. Wuttig, Thin Solid Films, **408**, 310 (2002).
[4] J. Rocca, M. Eraz, M. Fontana, B. Arcondo, Journal of Non-Crystalline Solids, **355**, 2068 (2009).
[5] Dong Hun Kim, Myung Sun Kim, Ran-Young Kim, Kyung Sun Kim, Ho Gi Kim, Materials Characterization, **58**, 479 (2007).
[6] Tong Ju, John Viner, Heng Li, P. Craig Taylor, J. of Non-Cryst. Solid, **354**, 2662 (2008).
[7] V. Pamukchieva, A. Szekeres, Optical Materials, **30**, 1088 (2008).
[8] J. Prikryl, M. Hrdlicka, M. Frumar, J. Orava, L. Benes, Journal of Non-Crystalline Solids, **355,** 1998 (2009).
[9] A. A Piarristeguy, E. Barthélémy, M. Krbal, J. Frayret, C. Vigreux, A. Pradel, Journal of

Non-Crystalline Solids, **355**, 2088 (2009).
[10] J. Bicerano, S. R. Ovshinsky, J. Non-Cryst. Solids, **74**, 75 (1985).
[11] F. Demichelis, G. Kaniadakis, A. Tagliafferro and E. Tresso, ``Applied Optics``, **26**(9), 1737 (1987).
[12] A. R. Hilton, D. J. Hayes and M. D. Rechtin, J. Non-Cryst. Solids, **17**, 319 (1975).
[13] L. Pauling, "The nature of chemical bond" 3rd Ed, (Cornell University press), 91, New York (1960).
[14] A. L. Allred, J. Inorg. Nucl. Chem., 17(1961) 215.
[15] J. S. Sanghera, J. Heo, J. D. J. Machkenzie, J. of Non-Cryst. Solid, **103**, 155 (1988).
[16] Afaf A. Abd El-Rahman, M. Eid, A. Sanad, R. M. El-Okr, J. of Phys. Chem. Solids, **59**, 5 (1998).